Actuator forces in CFD: RANS and LES modeling in OpenFOAM

P. Schito, A. Zasso
Department of MechanicalEngineering – Politecnico di Milano, via La Masa 1, 20156 Milano, Italy

E-mail: paolo.schito@polimi.it

Abstract. Wind turbine wakes are a very challenging topic for scientific computations, but modern CFD frameworks and latest HPC centers allow setting up numerical computations on the wake induced by the wind turbine. The main issues is that the correct modeling of the wake is related to the correct modeling of the interaction between the blade and the incoming flow. The aim of the proposed work is to estimate the aerodynamic forces acting on the blades in order to correctly generate the rotor wake applying equivalent aerodynamic force source on the flow. The definition of a blade forces is done developing a model able to correctly estimate this aerodynamic forces as a function of the local flow seen by the blade during its revolution.

Introduction

The numerical method is implemented as an actuator-line approach in the open-source framework OpenFOAM®[1]. The key point of the problem is the correct definition of the wind incidence angle and wind speed that is responsible for the load on the blade. Standard approach relies on Blade Element Momentum theory to define the actual wind speed and incidence angle that produces a certain load. This approach is useful for structural calculations, but CFD provides very detailed flow fields that are useful for a more physical description of the local wind. Current AL models calculate the aerodynamic forces generated by a section of the blade, using as reference the wind evaluated in a single point, at some distance upstream of the rotor plane [2] or located in the region close to the blade section [3] [4]. These methods are quite diffused, however the results in terms of wind turbine power prediction can be improved; in general the thrust acting on the rotor is reproduced with a good accuracy.

The goal of this paper is the definition of a model able to define the relationship between flow characteristics around a wind turbine blade section and the forces acting on the airfoil: this model will be called Effective Velocity Model, since it aims to evaluate from local inflow velocity fields the equivalent undisturbed velocity incident to the airfoil and then use this value to correctly interpolate the airfoil tabulated polar curve and define the forces acting on the blade section.

Effective Velocity Model

As said in IEA Task 29 final report the principal variable in ALM implementation consist the angle of the angle of attack (AOA) defined as the geometrical angle between the undisturbed flow direction and the chord line and the effective velocity on the rotor plane, these because the normal and tangential force distribution on the blades are directly related to this two variable and transitively turbine torque, thrust and wake depend on force distribution.

The concept of the Effective Velocity Model (EVM) is to effectively use the big amount of information provided by CFD about the flow around an airfoil: calculating numerically the flow it is possible to evaluate the velocity on any point located around the wind turbine blade in order to get the information about the incoming wind and therefore it will be possible to insert the correct aerodynamic forces in the flow field using a method that uses this information.
The principal hypothesis in EVM development is that it is more effective to evaluate AOA and effective velocity on the rotor plane not sampling a single point but through the average of velocity sampled on a segment, and thus on multiple points, positioned perpendicular to the mean relative velocity direction
The main issue about EVM is the definition of sample segment length and position and the evaluation of relationship between the generated aerodynamic forces and flow sampled on this segment.

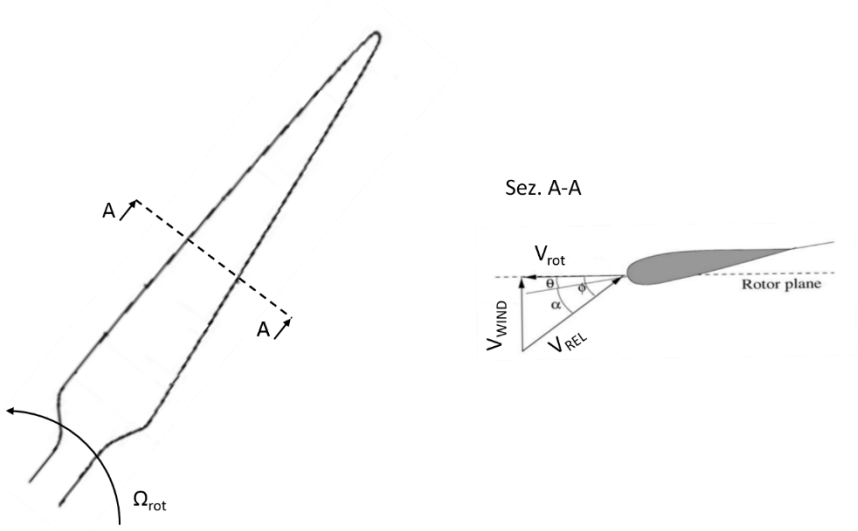

Figure 1. Identification of the airfoil on the rotating blade and generic airfoil on section A-A

The synthesis of the EVM is done looking at a generic 2D plane perpendicular to the rotating blade section A-A in figure 1, where α is the local angle of attack different to AOA for the effect of the induced velocity by the bound vortex generated by the airfoil [5]. In this plane the actuator line (AL) collapses in a punctual application of force becoming an ActuatorForce (AF) model of blade section. Referring to this generic section and choosing as blade profile a generic NACA0012 symmetric airfoil, a series of numerical simulations have been conducted for different angles of attack. The aim of these simulations was to set up the EVM in order to make it able to insert lift and drag forces as close as possible to the ones generated by the airfoil profile for every possible blade operational angle of attack.

Fluid dynamic equivalence of NACA profile and ActuatorForce
The basis of the AL model is the equivalence of flow velocity field resultant from physical interaction with blade profile and from the insertion of an equivalent force source in incompressible stationary Navier-Stokes momentum equations, reported in equations 1-2 neglecting turbulence modelling. A NACA0012 symmetric profile, with a chord length *c=1m* was taken for this analysis. Two simulations have been carried out, the first with a mesh modelled around the NACA 0012 profile (and hereafter named *NACA0012*) and the second with a regular and coarse mesh with AF force source (that is called *AF*) where the grid is completely Cartesian, with a mesh size equal to *1m*, that is the length of the profile chord. The total domain extension for both calculations is *50x50m*, and the airfoil is placed in the center of the domain. The simulations are set-up by performing a 2D set of simulation on different

meshes: the *NACA0012* mesh has 430000 cells, with 100 grid points along the airfoil chord and cell size increases with the distance from the airfoil as can be inferred in figure 2, while the AF mesh has uniform cell size and a total of 2500 cells as can be seen in figure 3. Steady-state RANS equations were solved using a *k-ω-SST* turbulence model. In the numerical simulations the boundary velocity magnitude $V_\infty=10m/s$ is fixed, while the boundary velocity angle $\alpha_\infty = 10°$ that is the *AOA* fixed as boundary condition. On NACA0012 simulations the force on the airfoil was measured by integrating the pressure over the airfoil surface, see figure 4, while in AF calculations the force measured in the NACA0012 is directly introduced in the domain. In figure.5 the force inserted on the cell where the airfoil is located, is splitted in its component F_x and F_y along x and y axes.

$$\nabla \cdot \rho \boldsymbol{UU} - \nabla \cdot \mu \nabla \boldsymbol{U} = -\nabla \mathrm{p} \qquad \boldsymbol{U}_{airfoil\ wall} = \boldsymbol{0} \qquad (1)$$

$$\nabla \cdot \rho \boldsymbol{UU} - \nabla \cdot \mu \nabla \boldsymbol{U} + \boldsymbol{f} = -\nabla \mathrm{p} \qquad \boldsymbol{f} = airfoil\ aerodynamic\ force \qquad (2)$$

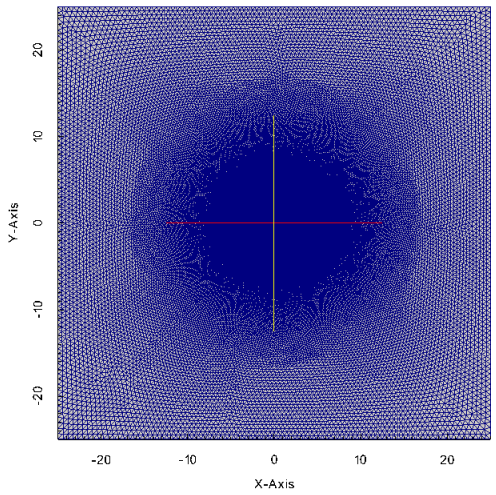

Figure 2. NACA0012 mesh.

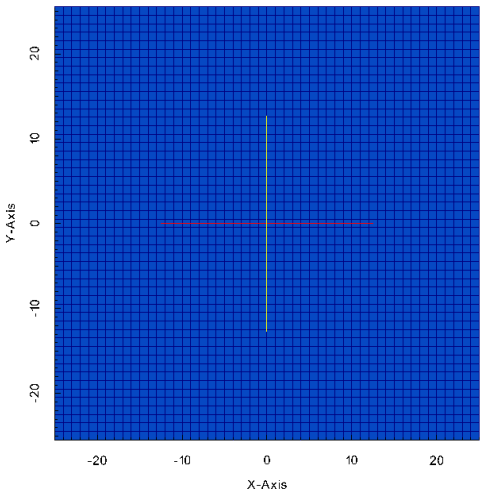

Figure 3. AF mesh.

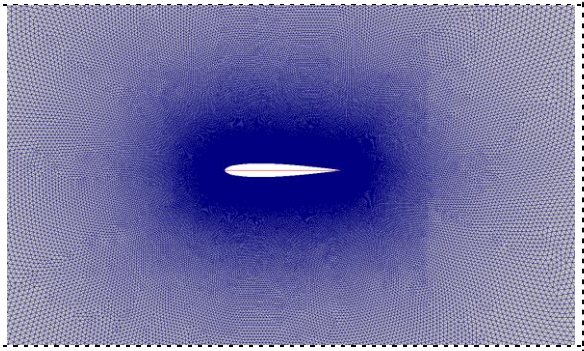

Figure 4. *mesh around NACA0012 airfoil*

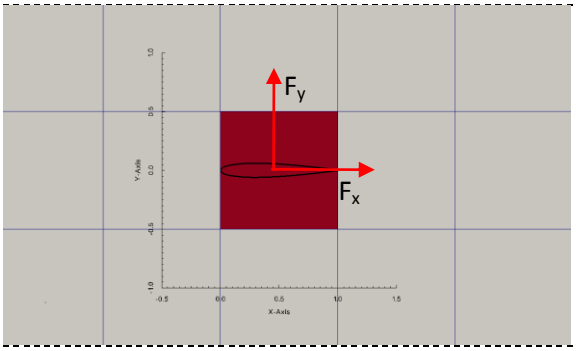

Figure 5. *mesh around AF insertion force cell, the position yields by NACA0012 airfoil is reported*

The first step in EVM validation work is to confirm the effective equivalence of velocity field from NACA0012 modelling, $\vec{V}_{\mathrm{NACA}}$, and AF analysis, $\vec{V}_{\mathrm{AF}}$.
The NACA0012 simulation has been evaluated and taken as benchmark for AF result, from NACA simulation the polar curve for this blade profile is extracted, this information is then used in AF simulation, fixed the angle of attack by boundary condition, while the correct aerodynamic force is inserted interpolating the aerodynamic coefficients and the correspondence between $\vec{V}_{\mathrm{NACA}}$, and $\vec{V}_{\mathrm{AF}}$ is analysed.

Distribution of force

As reported in several previous works [2] [4] [6] [7] the AF aerodynamic forces need to be distributed smoothly on several mesh points in order to avoid singular behaviour. In practice the aerodynamic blade forces are spatially distributed with a 2-dimensional normal distribution

$$f(x) = \frac{1}{\sqrt{(2\pi)^2 \cdot \epsilon^4}} \cdot e^{-\frac{1}{2}\frac{d^2}{\epsilon^2}} \tag{3}$$

Being d the distance between cell-centered grid points and the points where the actuator point lies, the ϵ parameter defines the shape of normal distribution function.

In this work the value of ϵ is studied to find the narrowest kernel function that prevents the occurrence of a singular numerical behaviour.

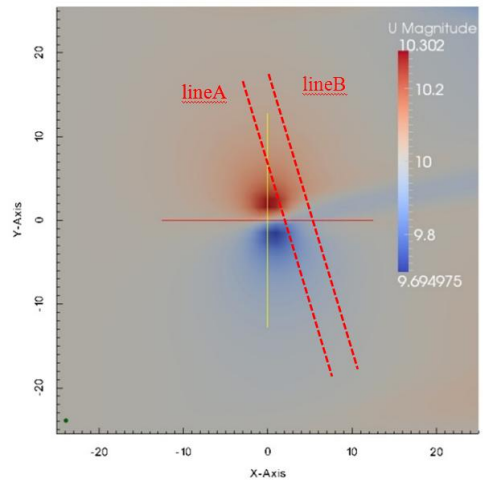

Figure 5. AF ε value study. Boundary conditions: $V_\infty = 10m/s$; $\alpha_\infty = 10°$.

The wake generated by AF for ϵ equal to 0.5,1 or 2 times the length of computational mesh size is sampled on the two control lines placed 2 and 5 chord length, equal to 1m, behind NACA0012 profile and AF point, those line are shown in figure 5.

In Figure 7 and Figure 8 the velocity magnitude and angle of AF simulation with different ϵ value, V_{AF} and $\sphericalangle\vec{V}_{AF}$ are plotted together with velocity magnitude and angle of NACA0012 simulation V_{NACA} and $\sphericalangle\vec{V}_{NACA}$ .versus line extension from upper point.

For smaller ϵ and consequently narrower spatial distribution of force the AF wake reproduces better the local shape of NACA0012 wake, however it is visible a spatial oscillation in the velocity and the angle for ϵ equal to *0.5*: the solver is steady state and the simulation reached convergence, therefore these oscillations have no physical motivation and have consequently only numerical explanation. To avoid this numerical oscillation, $\epsilon = 1$ was chosen and this value is used for all the following simulations.

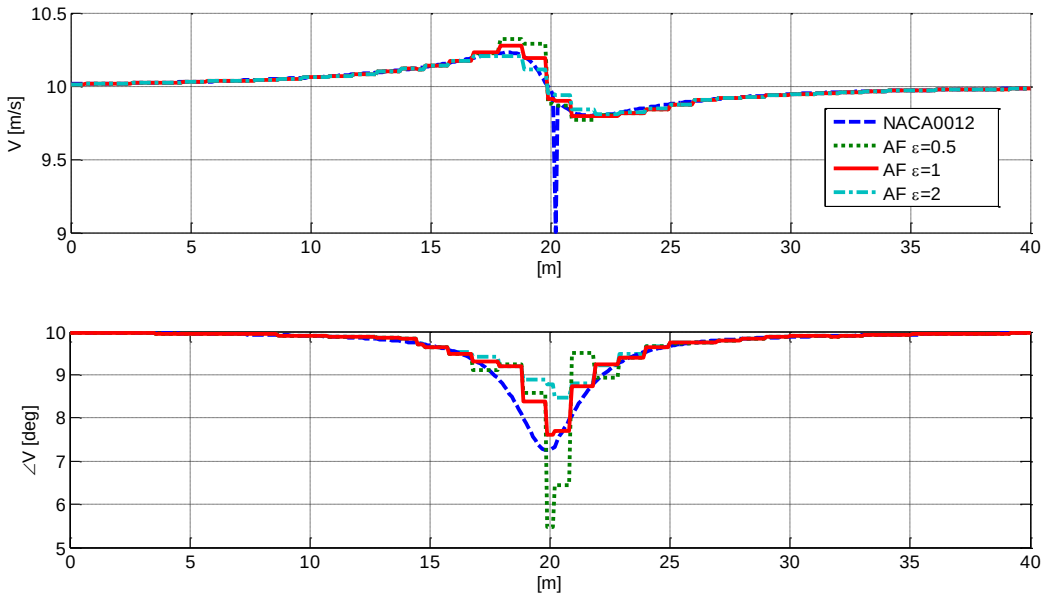

Figure 7. Wind velocity (V) and angle ($\measuredangle V$) sampled on line A for ϵ=0.5, 1 and 2

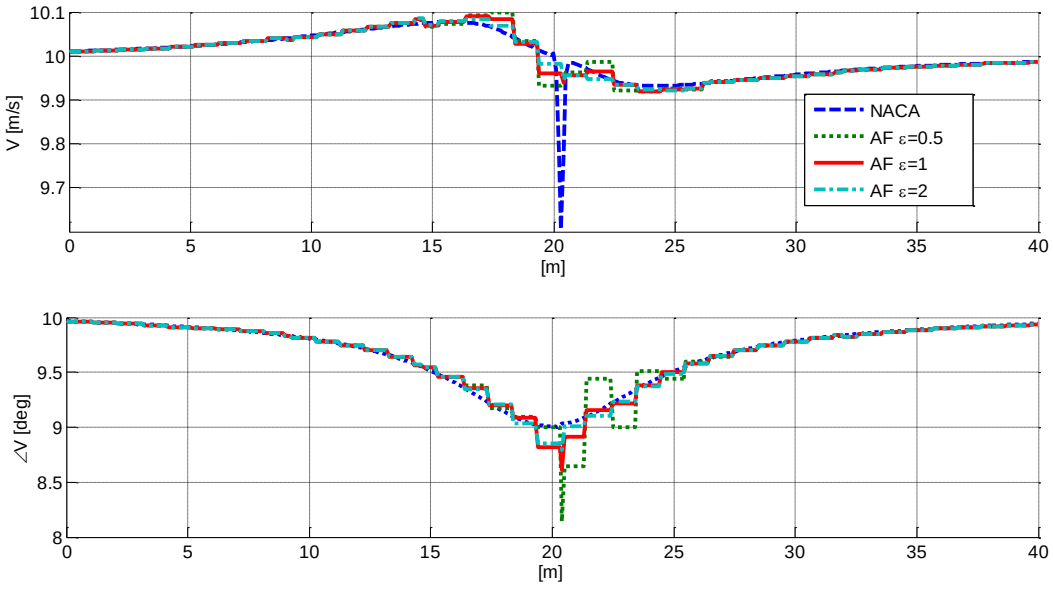

Figure 8. Wind velocity (V) and angle ($\measuredangle V$) sampled on line B for ϵ=0.5, 1 and 2.

Defined the regularization kernel extension a point to point comparison between the flow field calculated using the geometrical reproduction of the NACA profile V_{NACA} and the flow field calculated using the Actuator Force approach V_{AF}.is proposed: the result of NACA profile simulation has been interpolated for the cells of AF simulation, then the error between the two was calculated.

The relative $error^{i}_{v;\measuredangle(\vec{V})}$,computed for every AF simulation cell for both magnitude and phase, equations 3-4, is globally small and increases only in the region very close to the airfoil as can be observed in Figure 9 and Figure 10.

$$error_v^i = \left| \frac{(V_{AF}^i - V_{NACA}^i)}{V_{NACA}^i} \right| \quad (3)$$

$$error_{\sphericalangle(\vec{V})}^i = \left| \frac{(\sphericalangle\vec{V}_{AF}^i - \sphericalangle\vec{V}_{NACA}^i)}{\sphericalangle\vec{V}_{NACA}^i} \right| \quad (4)$$

Where V^i_{AF} and $\sphericalangle\vec{V}^i_{AF}$ is velocity field magnitude and angle computed on the i^{th} cell for AF simulation,

V^i_{NACA} and $\sphericalangle\vec{V}^i_{NACA}$ is velocity field magnitude and angle computed by NACA simulation averaged on the i^{th} cell of AF simulation.

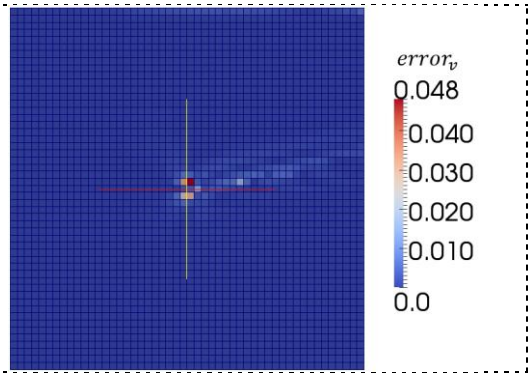

Figure 9. Magnitude absolute relative error

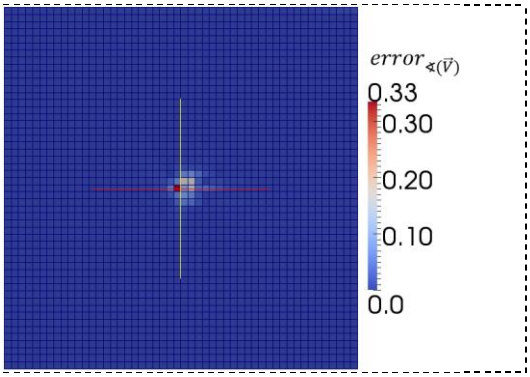

Figure 10. Phase absolute relative error

EVM definition

The tuning of EVM is based on the equality of the flow fields between the simulation of the full blade airfoil and the one related to the AF. The goal is to define the sample line through which the incoming velocity is evaluated and then the forces are calculated. The first step involves the definition of the sampling line length and its position in the computational domain relating to the AF point. Through the comparison between the full blade section case and the AF simulation, the analysis focuses on the velocity field in the region upwind of the profile.

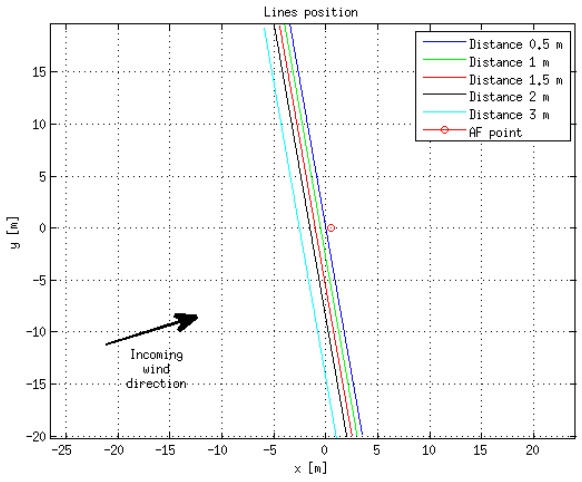

Figure 11. Position of the different sampling lines in the computational domain. The position of the AF point is marked by the circle

In Figure 11 different lines perpendicular to the undisturbed incident wind, placed a different distance from the cell-centre of the cell which the AF point belongs and crossing the entire domain, are used to collect data and compare the differences on the velocity field in terms of magnitude and angle, plotted in Figure 12 versus s, line extension from upper point.

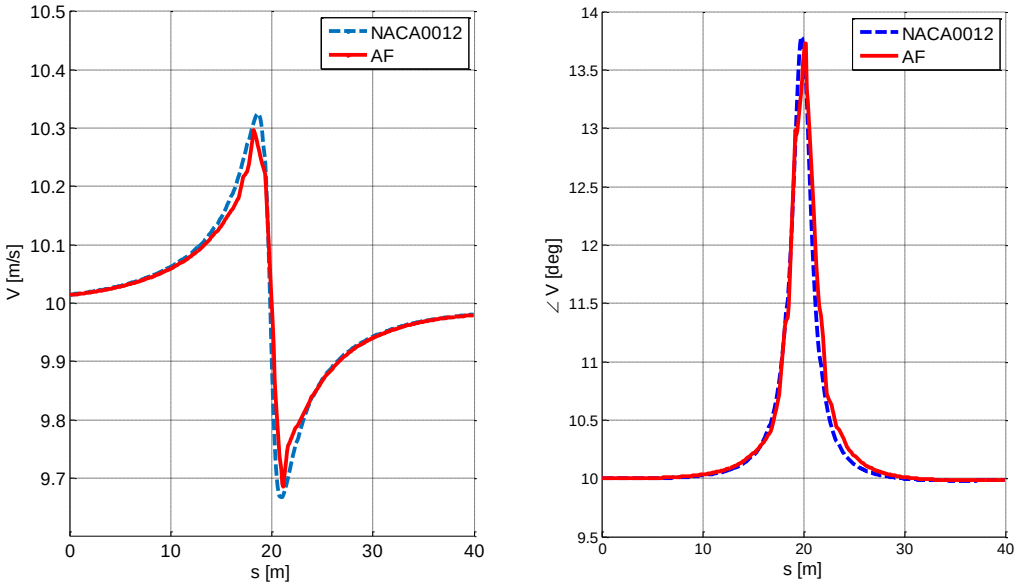

Figure 12. Comparison between the velocity calculated on NACA0012 and AF simulations in terms of magnitude (left) and angle (right), detected on the line placed 1.5 m in front of the AF point.

In order to establish the best position for the sampling line of the EVM the relative errors in magnitude $error_v(s,d)$ and phase $error_{\sphericalangle(\vec{V})}(s,d)$ between $\vec{V}_{\mathrm{NACA}}(s)$ and $\vec{V}_{\mathrm{AF}}(s)$, sampled on line at different distance form AF point, have been calculated.

$$error_v(s,d) = \left| \frac{(V_{AF}(s) - V_{NACA}(s))}{V_{NACA}(s)} \right|_{on\ sampling\ \ line\ distance\ =d} \quad (5)$$

$$error_{\sphericalangle(\vec{V})}(s,d) = \left| \frac{(\sphericalangle\vec{V}_{AF}(s) - \sphericalangle\vec{V}_{NACA}(s))}{\sphericalangle\vec{V}_{NACA}(s)} \right|_{on\ sampling\ \ line\ distance\ =d} \quad (6)$$

The mean error on the line is then evaluated especially taking into account the phase error, the tested AF case shows that a good compromise between the error values and the distance of the line, that should be as close as possible to better represent the instantaneous velocity value investing the AF point, is reached when the sampling line is positioned at a distance equal *1.5*chord lengths, as can be deduced from the plot of Figure 13.

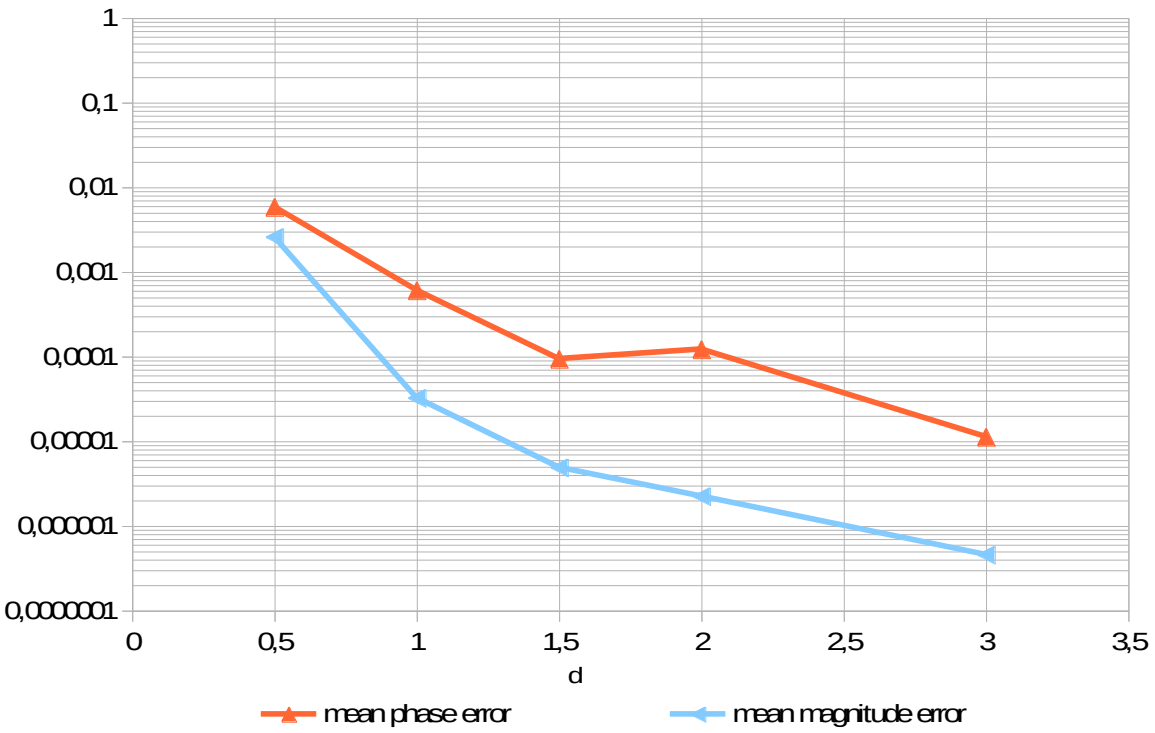

Figure 13. Comparison between the NACA0012 and the AF simulations on U (magnitude and angle) function of the coordinate s, detected on the line placed 1.5 m in front of the AF point.

The second step deals again with a comparison between the airfoil NACA and the AF, but the purpose now is the definition of the length of the EVM sampling line. Focusing on the chosen line placed at a distance of 1.5 m upstream the AF point and set a new coordinate q (representative of the portion of the line that is considered), a new examination of the two simulations is done. For each value of q, between 0 and the total length of the line, the variation in the incidence angle $\Delta\alpha$ is calculated, where

$$\Delta\alpha = mean\big(\alpha(q)\big) - \alpha_{\infty} \tag{6}$$

For both the NACA0012 and the AF simulations. The relative difference between the curves decreases increasing the portion of sampling line considered coordinate, because a long segment takes into account also the information given by the cells that are far from the airfoil position, where the air is very close to the undisturbed flow. Again a compromise is needed and through the analysis of the data reported in Figure 14, it is chosen a width of 5 times the mesh dimension for the EVM sampling segment. As can be seen by the mentioned plot for a segment of 5 m the descendant trend of the relative difference between NACA0012 and AF simulations is clearly visible. In Figure 15 the chosen position of the EVM sampling line in the computational domain respect to the AF point is represented.

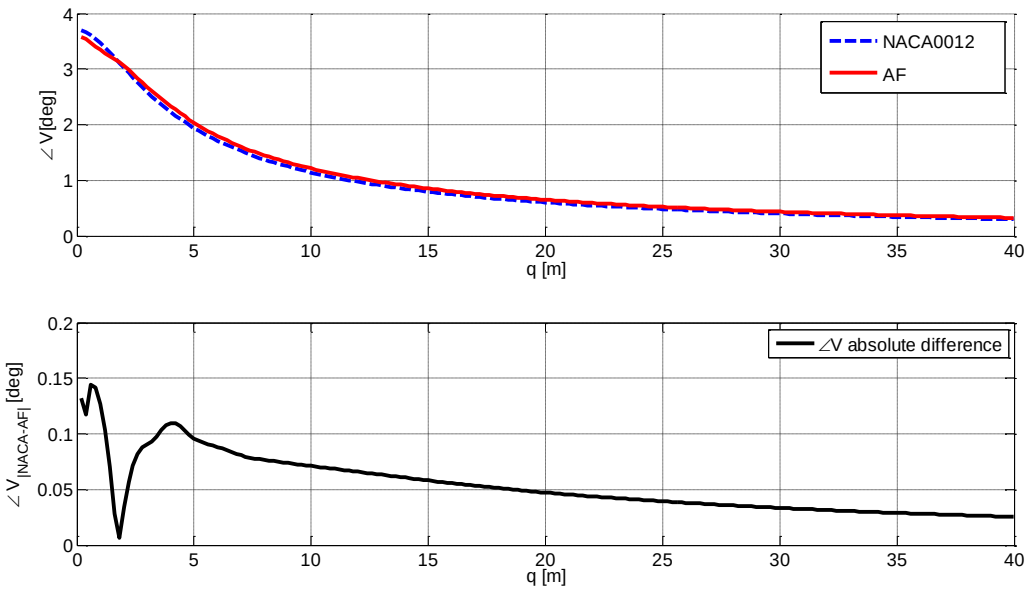

Figure 14. Difference between Δα and absolute difference between NACA0012 and AF data.

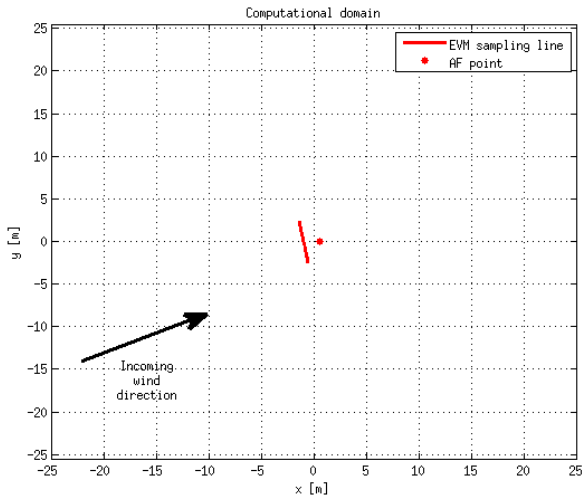

Figure 15. EVM line and AF position in the computational domain.

The aim of the third phase of the EVM construction is the definition of the empirical formula relating the angle detected by the EVM close to the profile and the undisturbed angle used to calculate and then to apply the aerodynamic forces delivered by the airfoil. The idea for this model is that the mentioned formula is given in terms of a correction that must be applied to the angle of α provided by the EVM; considering that the generic aerodynamic force (lift or drag) is defined as:

$$lift = \frac{1}{2}\rho U^2 C_l(\alpha_\infty)c \tag{7}$$

$$drag = \frac{1}{2}\rho U^2 C_d(\alpha_\infty)c \tag{8}$$

it is possible to suppose that the angle correction Δα relation is dependent on the parameters directly influencing the forces:

$$\Delta\alpha = \alpha_{EVM} - \alpha_{\infty} = \Delta\alpha(C_l, C_d, {}^{c}/_{M}) \tag{9}$$

Where α_{EVM} is the calculated angle of attack from EVM, α_{∞} is the boundary one equal to AOA, C_l and C_d are the aerodynamic coefficients of the considered airfoil and c is the chord length, M the mesh size, so c/M is a non-dimensional value. To quantify the Δα correction a large test campaign was made considering a large variation for all the comparing parameters: different test cycles were made to study the influence of varying C_l (within the cycle), while C_d and c/M were fixed for the considered cycle itself. Since the flow is stationary, the validation of the EVM just requests to compare the detected α_{EVM} with the undisturbed angle α_{∞}, that is known a priori. So here are presented the different tests made:

- C_l varying in the range from 0 to 2, step 0.2, with C_d fixed once equal to 0, once equal to 0.25, once equal to 0.5;
- fixed $C_l = 1$, $C_d = 0$, a test cycle was made varying the profile chord from 0.1 to 1, step 0.1.

These tests give an idea of the influence of the parameter c/M, even if it is quite obvious the linear influence of this parameter, because the forces depend linearly by c, when C_l, C_d and U are fixed.

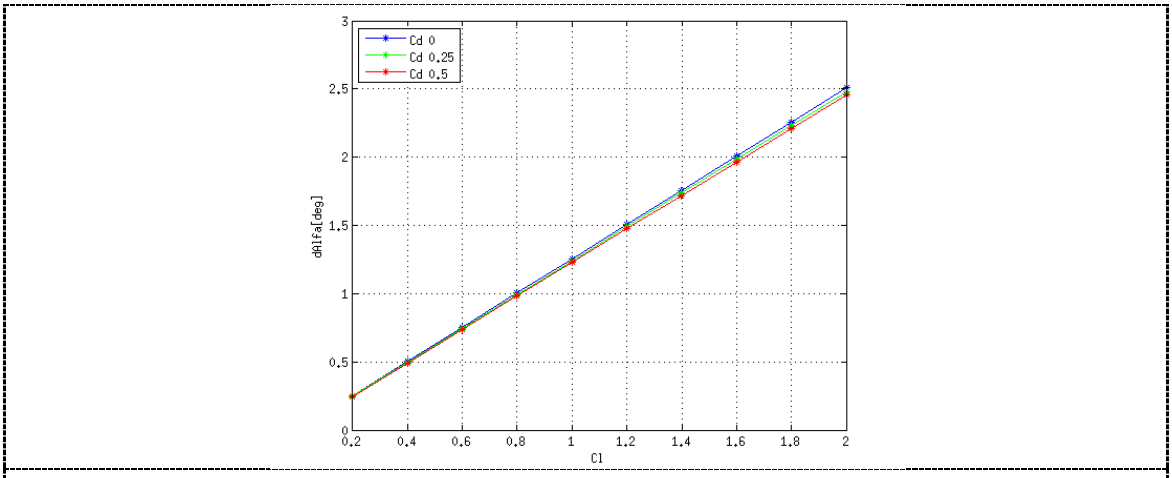

Figure 16. Influence of C_l and C_d on Δα value.

For all tests M was equal to 1 m and the initial condition for V is horizontally directed, magnitude of 10 m/s. Relating to Figure 16 the following evidences are detected and used to definitively estimate the EVM correction:

- $\Delta\alpha(C_l)$ is a linear function;
- the correction depends primarily by C_l, but the influence of C_d is clearly visible, as an alteration of the slope of $\Delta\alpha$ (C_l) line;
- the non-dimensional ratio c/M impact linearly to the Δα value.

Hence this is the proposed correction:

$$\Delta\alpha = {}^{c}/_{M} \cdot (1.2553 - 0.0552\, C_d)\, C_l \tag{10}$$

An important observation is that no correction is needed for the absolute value of V, since the presence of profile induces only a deflection on the incoming flow. Studies are made also in this direction and confirmed the hypothesis. Of course, must be reminded that the Δα correction previously presented is inextricably associated to the chosen position for the EVM sampling line.

The final step of the tuning of the EVM is a first validation of the introduced model. A new test campaign is set-up, considering a stationary case, V_{∞}=*10m/s* is keep fixed, while the boundary velocity

angle α_∞ sweep from -16° to 16°. The tests are made to show the robustness of the model for different angles of attack, considering also the stall condition. The EVM effectiveness is proven by the good agreements between forces generated by different NACA profiles and the ones calculated by AF. Figure 17 and Figure 18 show that the model works correctly with every type of airfoil, known polar curves simply, because the Δα correction is a function of non-dimensional coefficients.

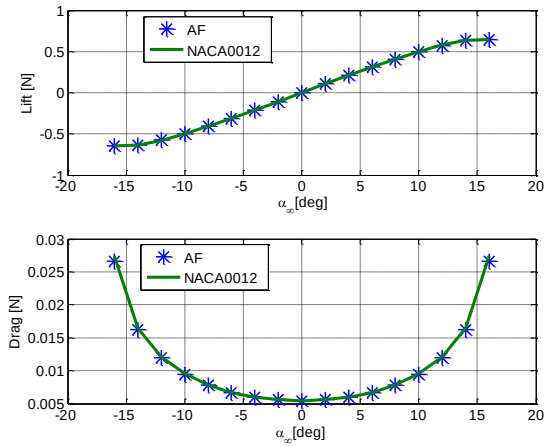

Figure 17. NACA0012 vs AF forces with EVM.

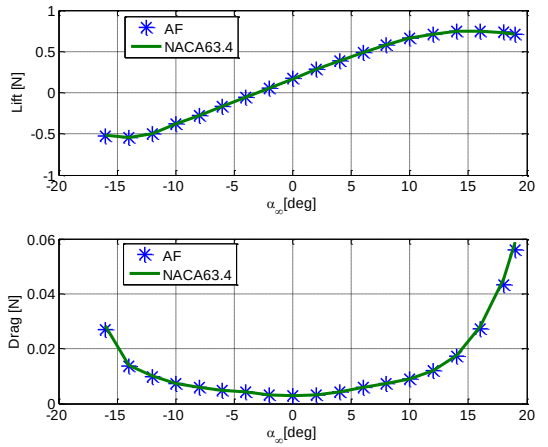

Figure 18. NACA63.4 vs AF forces with EVM.

Conclusion

The definition of an interaction model for introducing the aerodynamic forces using an actuator force approach has been studied on a two dimensional model, by comparing the results on a geometrically reproduced airfoil and using the actuator force approach.

The flow field upwind and downstream of the profile show a good agreement only if a suitable regularization kernel is applied: a small kernel suffers of numerical instabilities, while a too large kernel distributes widely the forces and cannot reproduce the near wake of the profile. An effective velocity model tuned on lift and drag correction allows to define correctly the forces generated on the airfoil, and therefore allows to reproduce not only the forces acting on the profile, but is able to generate a wake similar to the one of a geometrically reproduced airfoil.

Acknowledgments

The authors would like to thank Matteo Caccialanza and Luca Bernini for the help in conducting this research. The author thank also PRACE platform for funding the numerical analysis with Project 2012061147 - INCOME4WINDFARMS – Innovative Computational Methods for Wind Farms.

References

[1] The OpenFOAM Foundation, *www.openfoam.org*

[2] Wu Y, Porté-Agel F. *Large-eddy simulation of wind-turbine wakes: Evaluation of turbine parametrisations. Boundary - layer meteorology*. 2011;138(3):345-366.

[3] Martinez L, Leonardi S, Churchfield M, Moriarty P. *A comparison of actuator disk and actuator line wind turbine models and best practices for their use. In: American Institute of Aeronautics and Astronautics*; 2012. 10.2514/6.2012-900.

[4] Troldborg N. *Actuator line modeling of wind turbine wakes.* [PhD Thesis]. Technical University of Denmark, Lyngby, Denmark; 2008.

[5] Wen Zhong Shen, Martin O.L, Hansen and Jens Nørkær Sørensen. *Determination of the Angle of Attack on Rotor Blades*. 10.1002/we.277

[6] Sorensen JN, Shen. *Numerical modeling of wind turbine wakes.Journal of fluids engineering*. 2002;124(2):393-399.
[7] Ivanell. *Numerical computations of wind turbine wakes. Trita-MEK*. 2009.